Boundary critical behaviour of two-dimensional random Ising models

1998 J. Phys. A: Math. Gen. 31 2801

(http://iopscience.iop.org/0305-4470/31/12/006)

J. Phys. A: Math. Gen. **31** (1998) 2801–2814. Printed in the UK PII: S0305-4470(98)89266-4

Boundary critical behaviour of two-dimensional random Ising models

F Iglói†‡, P Lajkó‡, W Selke§ and F Szalma‡

† Research Institute for Solid State Physics, H-1525 Budapest, PO Box 49, Hungary
‡ Institute for Theoretical Physics, Szeged University, H-6720 Szeged, Hungary
§ Institut für Theoretische Physik, Technische Hochschule, D-52056 Aachen, Germany

Received 17 November 1997

Abstract. Using Monte Carlo techniques and a star–triangle transformation, Ising models with random, 'strong' and 'weak', nearest-neighbour ferromagnetic couplings on a square lattice with a (1,1) surface are studied near the phase transition. Both surface and bulk critical properties are investigated. In particular, the critical exponents of the surface magnetization, β_1, of the correlation length, ν, and of the critical surface correlations, $\eta_\parallel$, are analysed.

1. Introduction

Quenched randomness may have a profound effect on the nature of phase transitions. If there is a continuous phase transition in the perfect system then, according to the Harris criterion [1], the relevance of the perturbation is connected to the sign of the specific heat exponent α in the pure system. The two-dimensional random Ising model with $\alpha = 0$ represents the borderline case of the perturbational theory. Indeed, that model has been the subject of intense investigations to clarify its critical properties [2–4].

According to field-theoretical studies [2, 3] the randomness is, in the renormalization group sense, a marginally irrelevant perturbation, and therefore leads to logarithmic corrections to the power-law singularities of the pure model. For example, the bulk magnetization, m_b, and the correlation length, ξ, are expected to behave near the transition point as

$$m_b \sim t^{1/8} |\ln t|^{-1/16} \tag{1}$$

and

$$\xi \sim t^{-1} |\ln t|^{1/2} \tag{2}$$

where $t = |T_c - T|/T_c$ is the reduced temperature. The critical spin–spin correlation function $G(r)$ *averaged* over several samples has a pure power-law decay [5]

$$G(r) \sim r^{-1/4}[\mathcal{A} + \mathcal{B}/(\ln r)^{-2}] \tag{3}$$

whereas the *typical* correlation function calculated in a large single sample is conjectured [6] to decay as

$$G(r) \sim r^{-1/4}(\ln r)^{-1/8}. \tag{4}$$

The above conjectures are found to be in agreement with numerical results of large-scale Monte Carlo (MC) simulations [7, 4, 8] and transfer matrix calculations [9–11]. However,

0305-4470/98/122801+14$19.50

conflicting interpretations of the numerical findings have also been suggested, invoking dilution-dependent critical exponents and weak universality [12, 13].

In this paper, we consider the boundary critical behaviour of the two-dimensional random bond Ising model. The surface critical properties of the perfect model have been exactly known for many years [14]. For example, the asymptotic behaviour of the surface magnetization, m_1, and the correlation length, $\xi_\parallel$, measured parallel to the surface, is given by

$$m_1 \sim t^{1/2} \tag{5}$$

and

$$\xi_\parallel \sim t^{-1} \tag{6}$$

whereas the critical surface spin–spin correlation function has the asymptotic decay:

$$G_s(r) \sim r^{-1}. \tag{7}$$

Thus, the corresponding critical exponents are $\beta_1 = \frac{1}{2}$, $\nu_\parallel = 1$ and $\eta_\parallel = 1$. No field-theoretical results are available for the random case. However, it seems reasonable to expect, in analogy to the bulk properties, that the randomness is a marginally irrelevant variable at the surface fixed point as well. Then one might obtain logarithmic corrections to the asymptotic behaviour of the perfect model.

In this study, we performed extensive numerical investigations to illuminate this issue by determining the surface critical properties of the Ising model with nearest-neighbour random couplings on the square lattice. In our first approach, we used large-scale MC techniques and computed the surface magnetization and the complete magnetization profile of the model. Our second method is based on the star–triangle (ST) transformation. By that method we calculated both the surface magnetization and the surface correlation function of the model. By the two, in several respects complementary approaches, we determined numerically the complete set of surface critical exponents, including the surface magnetization exponent β_1, the correlation length exponent $\nu_\parallel$ and the decay exponent of the critical suface correlations $\eta_\parallel$. Note that some of the MC results on the surface magnetization have already been announced in [15].

This paper is organized as follows. The MC results on the surface magnetization and the magnetization profiles are presented in section 2. In section 3 we describe the ST approach as applied to the random Ising model and discuss the numerical results on the surface magnetization and the surface correlation function. The main conclusions are given in section 4. Some details of the ST method have been transferred to the appendix.

2. Monte Carlo simulations

Let us consider the Ising model with nearest-neighbour ferromagnetic couplings, where the spins $s_{i,j}(=\pm 1)$ are situated on the sites (i, j) of a square lattice. A surface may be introduced by cutting the coupling bonds along one of the axes of the lattice, leading to the (10) surface, or along the diagonal, leading to the (11) surface. In the MC simulations, we studied systems with two parallel surface lines, each line having L sites. Each row perpendicular to the surface consists of K sites. The spins in the first and last row are assumed to be connected by periodic boundary conditions. The lines parallel to the surfaces are numbered by the index i, i.e. $i = 1$ and $i = K$ denote the two surface lines. The index j refers to the position along a line, running from 1 to L. The total number of spins is $K \times L$. The aim of the simulations is to determine thermal properties of the semi-infinite system, where $K, L \longrightarrow \infty$; therefore finite-size effects need to be studied with care.

The interaction between neighbouring spins may be either 'strong', $J_1 > 0$, or 'weak', $0 < J_2 < J_1$. Strong and weak couplings are distributed randomly, with p (or $1 - p$) being the probability of a weak (or strong) bond. If both interactions occur with the same probability, $p = \frac{1}{2}$, then the model is self-dual [16]. The self-dual point is located at

$$\tanh(J_1/k_B T_c) = \exp(-2J_2/k_B T_c) \tag{8}$$

determining the critical temperature, T_c, of the bulk Ising system ($K, L \longrightarrow \infty$, and full periodic boundary conditions) if the model undergoes one phase transition. Indeed, results of previous simulations support that assumption [4, 7]. The simulations were carried out for the self-dual case, i.e. at $p = \frac{1}{2}$.

Certainly, one expects that both bulk and surface will still order at the bulk critical temperature, T_c, in a two-dimensional model with short-range interactions. The one-dimensional surface does not support any separate ordering, so that one encounters the 'ordinary transition' [17, 18].

Varying, in the self-dual case, the ratio of the strong and weak couplings, $r = J_2/J_1$, one may change the degree of dilution. At $r = 1$, one recovers the perfect Ising model, while $r = 0$ corresponds to the percolation limit, where $T_c = 0$. As has been shown before [7], the crossover to the randomness-dominated bulk critical behaviour may be monitored conveniently by choosing r in the range of $\frac{1}{10}$ to $\frac{1}{4}$. Then the crossover length, at criticality, ranges from a few to about 20 lattice spacings [7]. Indeed, we simulated the random model at these two values, $r = \frac{1}{4}$ and $\frac{1}{10}$, augmented by computations for the perfect model, $r = 1$.

Most of the simulations were performed for the (11) surface, albeit some runs were also completed for the (10) surface to compare with exact results. For the (11) surfaces, we usually set $L = K/2$, with K ranging from 40 to 1280 to check for finite-size effects. For the (10) surfaces, quadratic systems were studied. We averaged over an ensemble of bond configurations (or realizations). The number of realizations typically ranged from at least 15 for the largest systems up to several hundred for the small systems. In general, the one-cluster flip MC algorithm was used (mainly for testing purposes, we also applied the single-spin–flip method) generating, close to the critical point, several 10^4 clusters per realization. Note that the statistical errors for each realization were significantly smaller than those resulting from the ensemble averaging. To avoid inaccuracies due to a, possibly, unfortunate choice of the random-number generators, we compared results obtained from shift register and linear congruential generators.

The crucial quantity, computed in the MC simulations, is the magnetization profile. It is described by the magnetization per line, $m(i) = \langle |\sum s_{i,j}| \rangle / L$, where $s_{i,j}$ denotes the spin in line i and row j, with $i = 1, 2, \ldots, K$, and summing over $j = 1, 2, \ldots, L$. The absolute values are taken to obtain a non-vanishing profile for finite systems, as usual. The surface magnetization is given by $m_1 = m(1) = m(K)$.

Because the distribution of the random bonds is the same in the bulk and at the surface, one may expect a monotonic decrease of $m(i)$ on approach to the surface, due to the reduced coordination number at the surface (being two for the (11) and three for the (10) surface). This behaviour is illustrated in figure 1, comparing magnetization profiles of the perfect, $r = 1$, and random, $r = \frac{1}{4}$, Ising model with a (11) surface, at the same distances from T_c, measured by the reduced temperature $t = |T - T_c|/T_c$. The critical point, T_c, follows from (1). Obviously, randomness tends to suppress the magnetization, at a fixed value of t. The profiles display a pronounced plateau around the centre of the systems, at which the bulk magnetization, m_b, is reached. The existence of the broad plateau indicates that the linear dimension K of the MC system is sufficiently large to compute, for instance, the surface magnetization of the semi-infinite system. Of course, in addition, one has to

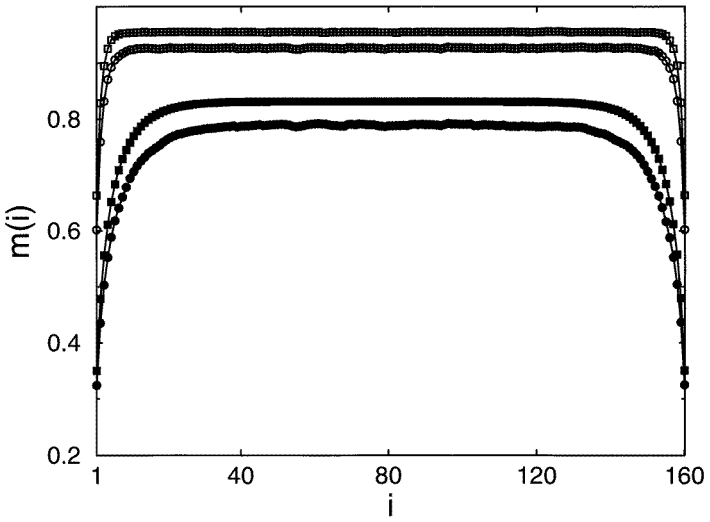

Figure 1. Magnetization profiles $m(i)$ of two-dimensional perfect (squares) and random, $r = \frac{1}{4}$ (circles), Ising models with (11) surfaces, at $t = 0.2$ (open symbols) and $t = 0.05$ (full symbols). Systems of size 160×80 were simulated.

monitor possible changes of m_1 with L, thereby having possible finite-size effects due to that dimension under control. Note that m_b is known exactly in the perfect case [14], and very accurately in the random case [7].

For the perfect two-dimensional Ising model with a (10) surface, the complete magnetization profile has been calculated exactly in the continuum limit [19, 20]. In particular, the profile approaches the bulk value in an exponential form, with $m_b - m(i) \propto \exp(-\mathrm{i}/\xi_r)$, where ξ_r is the bulk 'correlation range', which only becomes asymptotically, as $T \longrightarrow T_c$, identical to the bulk 'true correlation length' [21]. Indeed, we tested the accuracy of our simulational data by comparing them, for the (10) surface, to the exact expression. In addition, we found that the same correlation range determines the exponential approach of the magnetization towards its bulk value in the (11) case as well.

For the perfect two-dimensional Ising model with a (11) surface, exact results exist for the surface magnetization, m_1, and the magnetization in the next line, $m(2)$ [22]. Again, the MC data, obtained with modest computational efforts, agreed very well with the exact results, as shown in figure 2. In the figure, the 'effective exponent' $\beta(i)_{\mathrm{eff}}$ is depicted, defined by

$$\beta(i)_{\mathrm{eff}}(t) = \mathrm{d}\ln(m(i))/\mathrm{d}\ln(t). \tag{9}$$

Certainly, as $t \longrightarrow 0$, the effective exponent acquires the true asymptotic value of the critical exponent $\beta(i)$. For example, the asymptotic critical exponent of the surface magnetization is $\beta(1) = \beta_1 = \frac{1}{2}$, being, incidentally, identical for (11) and (10) surfaces. Because the magnetization $m(i)$ is computed at discrete temperatures t_k, we use in analysing the simulational data, instead of (9) the corresponding difference expression, with $t = (t_k + t_{k+1})/2$. The error bars, included in figure 2, have been calculated in a conservative fashion, getting the bounds for β by comparing the upper (lower) limit of $m(i)$ to the lower (upper) limit of $m(i+1)$, where the bounds of the magnetization are computed in the standard way from the ensemble averaging. Alternately, we also computed the error bars from usual error propagation, which turned out to be appreciably smaller.

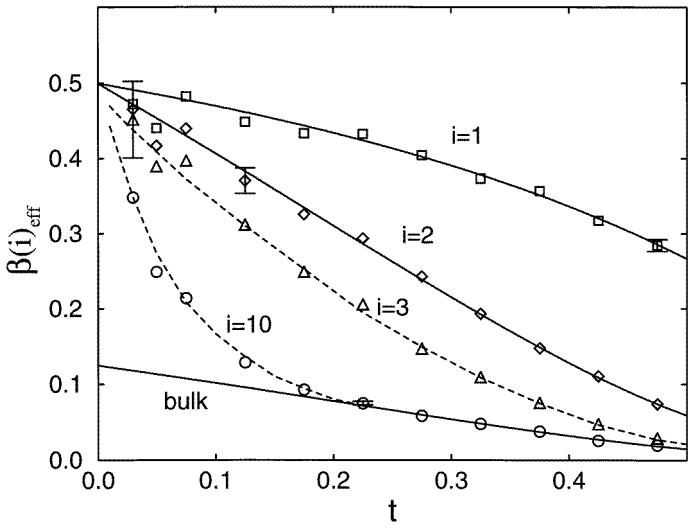

Figure 2. Effective exponent $\beta(i)_{\rm eff}$, with $i = 1, 2, 3$, and 10, versus reduced temperature t, for the perfect Ising model with (11) surface. The full curves denote exact results [14, 22]. MC data for systems of sizes 80×40 ($t > 0.3$), 160×80 ($0.07 < t < 0.3$), and 320×160 ($t < 0.07$) are shown.

In figure 2, the temperature dependence of the effective exponent $\beta(i)_{\rm eff}$ deeper in the bulk is also displayed. For example at $i = 10$, one readily observes the crossover from the bulk effective exponent (as follows from the exact expression for the bulk magnetization [14]) to the surface dominated behaviour, when the correlation length becomes large compared with the distance from the surface. In general, at finite and arbitrarily large distances to the surface, $\beta(i)_{\rm eff}$ will always converge, on approach to T_c, to the surface critical exponent, $\beta_1 = \frac{1}{2}$, and not to the bulk critical exponent, $\beta = \frac{1}{8}$. Analogous observations have been reported for three-dimensional Ising models with surfaces [23].

The main aim of the MC study has been to estimate β_1 in the random case. Results of the extensive simulations are summarized in figure 3, depicting the effective exponent $\beta(1)_{\rm eff}(t)$ at $r = \frac{1}{4}$ and $r = \frac{1}{10}$, compared with its exactly known form for the perfect case, $r = 1$. Typical error bars, increasing closer to criticality, are displayed, based on standard error propagation resulting from the variance in ensemble averaging of $m_1(t_k)$ and $m_1(t_{k+1})$. Data obviously affected by finite-size effects have not been included in the figure.

As seen from figure 3, at a fixed distance from the critical point, t, $\beta(1)_{\rm eff}$ rises systematically with increasing dilution, reflecting the decrease in m_1 with stronger randomness. However, asymptotically, $t \longrightarrow 0$, it is conceivable that the surface critical exponent will coincide in the perfect and dilute cases, with $\beta_1 = \frac{1}{2}$. Indeed, a reasonable estimate, both for $r = \frac{1}{4}$ and $r = \frac{1}{10}$, is $\beta_1 = 0.49 \pm 0.02$.

Thence, the simulations demonstrated that the critical exponent β_1 is rather robust against introducing randomness simultaneously in the bulk and at the surface. Note that β_1 remains $\frac{1}{2}$ too, when only the surface bonds of the two-dimensional Ising model are randomized as described above, but keeping a unique bulk coupling, as we confirmed in simulations. Interestingly enough, in the three-dimensional case, introducing random nearest-neighbour strong and weak surface bonds, but having only one interaction for the bulk couplings, seems to be an irrelevant perturbation as well, i.e. the surface critical exponent seems to be the same as for the perfect surface, $\beta_1 \approx 0.80$ [23]. This robustness may indicate

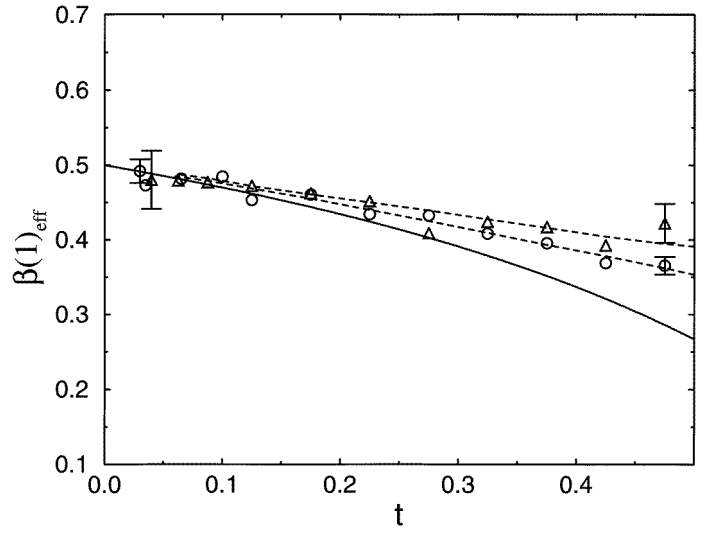

Figure 3. Effective exponent $\beta(1)_{\rm eff}$, versus reduced temperature t, for the random two-dimensional Ising model with (11) surface, at $r = \frac{1}{4}$ (circles) and $r = \frac{1}{10}$ (triangles). Systems of sizes 80×40 ($t > 0.3$), 160 × 80 ($t = 0.275$), 320 × 160 ($0.1 < t < 0.275$), 640 × 320 ($0.05 < t < 0.1$), and 1280 × 640 ($t < 0.05$) were simulated. The full curve denotes the exact result in the perfect case [22].

that the bulk critical fluctuations play a crucial role for the surface critical exponent, even though it is not determined by bulk critical exponents [17, 18]. If this is true, then our result for the two-dimensional case with random bulk and surface interactions suggests that the bulk critical fluctuations are not very sensitive towards dilution (in accordance with the theory of, at most, logarithmic modifications of the asymptotic power laws describing critical behaviour of the perfect system in two-dimensional Ising models [3, 4]). We shall come back to this aspect in the next section.

3. Star–triangle transformation

The star–triangle transformation was introduced by Hilhorst and van Leeuwen [24], and used later by others [25–27] to calculate the surface magnetization and the surface correlations in layered triangular lattice Ising models. Here we generalize the method for non-translationally invariant systems.

3.1. Star–triangle approach to boundary behaviour

The method is based on an exact mapping of the original triangular model, with couplings $\{K_1\}$, $\{K_2\}$ and $\{K_3\}$, to a hexagonal model with couplings $\{p_1\}$, $\{p_2\}$ and $\{p_3\}$ denoted by broken lines in figure 4. In the transformation the right-pointing triangles are replaced by stars such that the couplings are related by

$$K_1 = \frac{1}{4}\ln\left(\frac{\cosh(p_1+p_2+p_3)\cosh(-p_1+p_2+p_3)}{\cosh(p_1+p_2-p_3)\cosh(p_1-p_2+p_3)}\right) \tag{10}$$

and its cyclic permutation in the indices $i = 1, 2, 3$. In the second step of the mapping the left-pointing stars of the hexagonal lattice are replaced by triangles resulting in a new

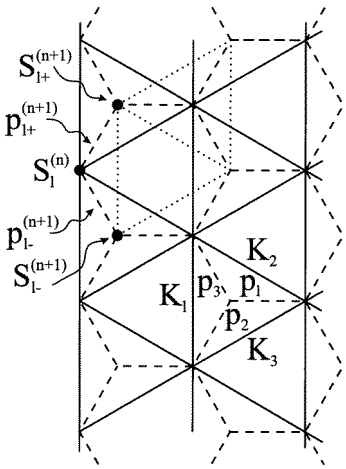

Figure 4. Mapping of the original triangular lattice (full line) to an equivalent hexagonal lattice (broken line) and further to a new triangular lattice (dotted line) using the ST transformation. The surface spins of the nth model ($S_l^{(n)}$) and those of the $(n+1)$th model ($S_{l+}^{(n+1)}$, $S_{l-}^{(n+1)}$) are connected by the surface couplings of the intermediate $(n+1)$th hexagonal model ($p_{l+}^{(n+1)}$, $p_{l-}^{(n+1)}$). The couplings $\{K_i\}$, $\{p_i\}$, $i = 1, 2, 3$ appearing in the ST relation in (10) are also indicated.

triangular lattice, which is denoted by dotted lines in figure 4. Iterating this procedure a sequence of triangular Ising models is generated ($n = 0, 1, 2, \ldots$) from the original model with $n = 0$.

As seen in figure 4, the surface spins of the nth and the $(n+1)$th models are connected by the surface couplings of the intermediate hexagonal model. In this geometry, the thermal average of the lth surface spin of the nth model, denoted by $\langle s_l^{(n)} \rangle \equiv \sigma_l^{(n)}$ is connected to the thermal averages of the neighbouring spins $s_{l-}^{(n+1)}$ and $s_{l+}^{(n+1)}$ of the $(n+1)$th model, where the corresponding surface couplings of the hexagonal lattice are denoted by $p_{l-}^{(n+1)}$ and $p_{l+}^{(n+1)}$. As shown in the appendix, one has

$$\sigma_l^{(n)} = a_{l+}^{(n+1)} \sigma_{l+}^{(n+1)} + a_{l-}^{(n+1)} \sigma_{l-}^{(n+1)} \tag{11}$$

where

$$a_{l+}^{(n)} = \tanh(p_{l+}^{(n)}) \frac{1 - \tanh^2(p_{l-}^{(n)})}{1 - \tanh^2(p_{l+}^{(n)}) \tanh^2(p_{l-}^{(n)})} \tag{12}$$

while in $a_{l-}^{(n)}$ one should interchange $p_{l+}^{(n)}$ and $p_{l-}^{(n)}$. Now using the vector notation $\boldsymbol{\sigma}^{(n)}$ for the surface spin exceptational values in the nth model and similarly $\boldsymbol{\sigma}^{(n+2)}$ for the $(n+2)$th model we obtain the relation

$$\boldsymbol{\sigma}^{(n)} = \mathbf{A}^{(n+1)} \mathbf{A}^{(n+2)} \boldsymbol{\sigma}^{(n+2)} \tag{13}$$

where the non-vanishing elements of the $\mathbf{A}^{(n+1)}$ matrix are given by $a_+^{(n+1)}(l)$ and $a_-^{(n+1)}(l)$ in terms of the surface couplings of the $(n+1)$th hexagonal lattice, equation (12), and a similar relation holds for $\mathbf{A}^{(n+2)}$. (We consider two successive steps in (13) in order to avoid complications with the different parity of the odd and even number of transformations.) Now taking the boundary condition $\lim_{n\to\infty} \boldsymbol{\sigma}^{(n)} = (1, , 1, \ldots, 1)$ we obtain for the average surface magnetization

$$m_1 = \lim_{L\to\infty} \frac{1}{L} \sum_{l=1}^{L} \sigma_l^{(0)} = \lim_{n\to\infty} f(n) \tag{14}$$

with

$$f(n) = \lim_{L\to\infty} \frac{1}{L} \sum_{i,j=1}^{L} \left[\prod_{k=1}^{n} \mathbf{A}^{(k)} \right]_{ij}. \tag{15}$$

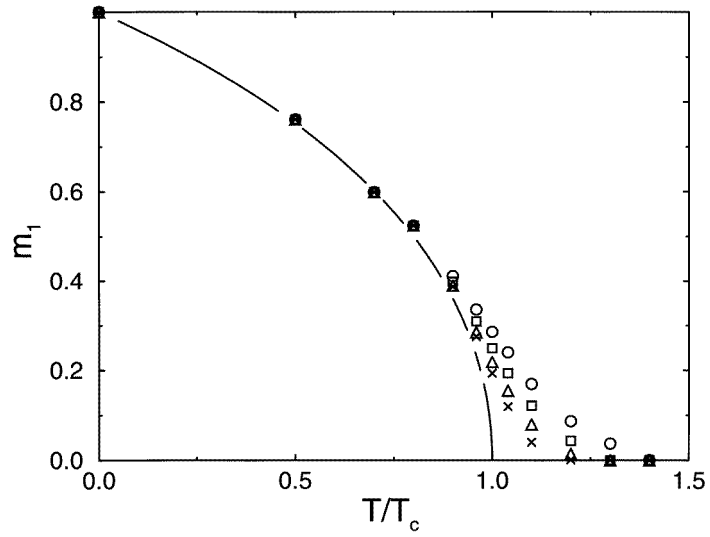

Figure 5. Magnetization of the $(1, 1)$ surface of the two-dimensional random Ising model with $r = \frac{1}{10}$ as a function of the temperature. The finite iteration approximants $f(n)$ of the ST method in equation (15) are indicated by circles ($n = 128$), squares ($n = 256$), triangles ($n = 512$) and by crosses ($n = 1024$). The asymptotic behaviour of $f(n)$ is different for $T < T_c$, $T > T_c$ and at $T = T_c$, as given in (18), (19) and (20), respectively.

We note that $f(n)$ in (15) is formally equivalent to the partition function of an n-step directed walk (polymer) in a random environment, where the (random) fugacities corresponding to the kth step of the walk are contained in the $\mathbf{A}^{(k)}$ matrix, which is just the transfer matrix of the directed walk.

Next we consider the average connected surface correlation function defined as

$$G_s(l) = \lim_{L\to\infty} \frac{1}{L} \sum_{i=1}^{L} [\langle s_{i+l} s_i \rangle - \langle s_{i+l} \rangle \langle s_i \rangle]. \tag{16}$$

As shown in the appendix, the surface correlations in the nth triangular model are connected to those in the $(n + 1)$th model, and the relation is given in terms of the surface couplings of the intermediate hexagonal lattice, equation (30), similarly to (11). Furthermore, as we argue in the appendix, in the asymptotic limit ($l \gg 1$) the surface correlation function can be expressed by the partition function $f(n)$ of the corresponding directed walk,

$$G_s(l) \propto \int_0^\infty \mathrm{d}n \, \frac{l}{n^{3/2}} \exp\left(-\frac{l^2}{n}\right) [f^2(n) - f^2(\infty)]. \tag{17}$$

Thus the surface properties of the model are connected to the asymptotic behaviour of $f(n)$ in (15). For different temperatures, corresponding to different thermodynamical phases of the random Ising model, the $f(n)$ function has different asymptotic behaviour, as can be seen in figure 5 for a dilution of $r = \frac{1}{10}$.

In the ordered phase, $T < T_c$, $f(n)$ approaches a finite limit, the surface magnetization m_1, through an exponential decay,

$$f^2(n) = m_1^2(T) + \mathcal{A} \exp(-n/4\xi_\parallel^2) \qquad T < T_c. \tag{18}$$

For $T \geqslant T_c$ the limiting value of $f(n)$ is zero, which corresponds to vanishing surface magnetization, and the decay for $T > T_c$ is exponential,

$$f(n) \propto \exp(-n/8\xi_{\parallel}^2) \qquad T > T_c \tag{19}$$

whereas *at the critical point*, it has the form of a power law

$$f(n) \propto n^{-\gamma} \qquad T = T_c. \tag{20}$$

We argue that $\xi_{\parallel}$ in equations (18) and (19) is the surface correlation length, below and above the critical point, respectively. Indeed, substituting (18) or (19) into (17) and evaluating the integral by the saddle-point method, we obtain

$$G_s(l) \propto \exp(-l/\xi_{\parallel}) \tag{21}$$

in accordance with the definition of the surface correlation length.

At the critical point, where $f(n)$ as in (20), the surface correlation function in equation (17) leads to a power-law decay $G_s(l) \sim l^{-4\gamma}$. Thus the decay exponent, $\eta_{\parallel}$, of the critical surface correlation function is given by

$$\eta_{\parallel} = 4\gamma. \tag{22}$$

We conclude at this point, that we have obtained a complete description about the surface properties of the random Ising model by the ST method. In the following, we shall use the above formalism to calculate numerically the surface magnetization, the critical surface correlations, and the correlation length.

3.2. Numerical results

In the actual calculations, we considered the random Ising model of the MC simulations, with a $(1, 1)$ surface, on a strip of width L of a diagonal square lattice (which can be considered as a triangular lattice with vanishing vertical couplings) and imposed periodic boundary conditions. To reduce finite-size effects, we considered relatively large strips (with L up to 512). We checked that the difference between the results for the two largest strips ($L = 256$ and $L = 512$) is essentially negligible, doing up to $n = 2000$ iterations†. We calculated the partition function $f(n)$ as a function of n, averaging over several (typically around twenty) random configurations of the couplings. The ratio r between the two, weak and strong, random couplings was chosen to be 1, $\frac{1}{4}$, and $\frac{1}{10}$, as in the simulations; both couplings occur with the same probability, $p = \frac{1}{2}$.

We start with the analysis of the results in the ordered phase, i.e. $T < T_c$. For a given temperature, $f(n)$ approaches the surface magnetization m_1, see (14), which is found to agree (within the error of the calculations) with MC data presented in the previous section. Approaching the critical point, the convergency of $f(n)$ with n becomes slower, in accordance with the form of the correction term in (18). Accordingly, accurate estimates become more difficult. As in the case of the simulations, the ensemble sampling over different configurations seems to be, however, the main source of error.

From the values for $m_1(t)$ at different reduced temperatures t, we determined effective surface magnetization exponents $\beta(1)_{\text{eff}}(t)$, as defined in (9). The estimates of the effective exponents obtained from the ST method are close to those found by the MC technique, see figure 3. Thus we confirm that β_1 is rather robust against introducing randomness in the two-dimensional Ising model.

† One expects that the characteristic values of n and L are related by $L \sim n^{1/2}$, like the size of transverse fluctuations of a directed walk to the number n of steps.

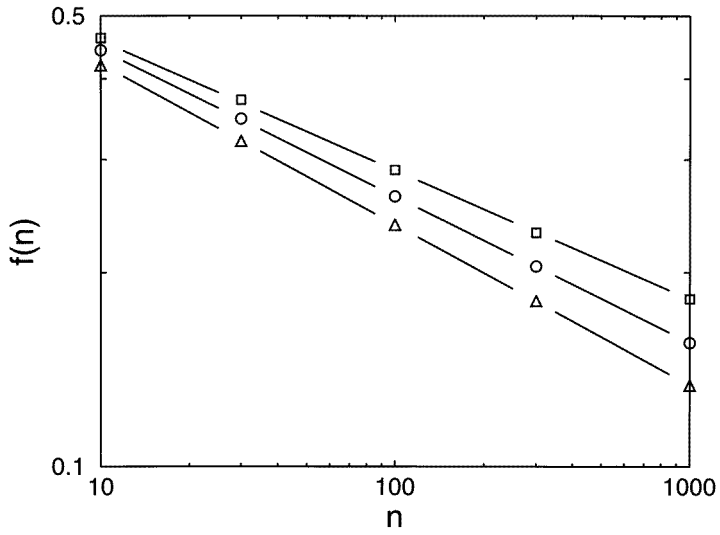

Figure 6. Finite iteration approximants to the surface magnetization, $f(n)$, as a function of n in a log–log plot, at the critical point of the two-dimensional random Ising model with dilution $r = \frac{1}{10}$ (squares) and $r = \frac{1}{4}$ (circles), compared with the perfect model (triangles). The slope of the curves, indicated by straight lines, is related to the average decay exponent $\eta_\parallel$ of the critical surface correlations through (22), see text.

At T_c, we studied the surface correlation function, as follows from the partition function $f(n)$. As shown in figure 6, $f(n)$ exhibits, with n ranging from 100 to 1000, on a log–log plot ($\ln(f(n))$ versus $\ln(n)$), an almost linear behaviour. The average slope then defines an average decay exponent $\gamma_{\rm av}$, see (20). For the perfect model, our estimate agrees nicely with the exact value $\gamma_{\rm pure} = \frac{1}{4}$. In the random case, the average exponent decreases with rising randomness, i.e. decreasing value of r. For $100 < n < 1000$, we obtain the average exponents $\gamma_{\rm av} = 0.228$ and $\gamma_{\rm av} = 0.207$, at $r = \frac{1}{4}$ and $r = \frac{1}{10}$, respectively. Based on these estimates, one may argue, that the decay exponent $\eta_\parallel$, see equation (22), also varies with dilution, r. However, a more detailed analysis is needed to substantiate or repudiate these statements. For instance, looking at the local effective exponent, defined in analogy to (9), a slight increase of that exponent with increasing n is observed. Indeed, the data for $f(n)$ depicted in figure 6, may be fitted by the power law of the perfect model, modified by logarithmic corrections with almost identical confidence (doing least-square fits) as by the power laws with the average, dilution dependent exponents. Thence, our data leave room to different interpretations.

In the disordered phase of the model, $T > T_c$, we studied the correlation length from the asymptotic decay of $f(n)$ in (19). Examples of the results of our calculations are shown in figure 7, plotting $\ln(f(n))$ as a function of n at several temperatures t for $r = \frac{1}{10}$. As seen from the figure, $f(n)$ seems to exhibit an exponential decay, with $\xi_\parallel(t)^{-2}$ following from the slopes of the curves. Approaching the critical temperature T_c, the correlation length is expected to diverge as $\xi_\parallel(t) \sim t^{-\nu}$. From data at $t > 0.05$, we calculated average critical exponents $\nu_{\rm av}(t)$, with $\nu_{\rm av} = 1.07(2)$ at $r = \frac{1}{4}$, and $\nu_{\rm av} = 1.13(6)$ at $r = \frac{1}{10}$. These average exponents are larger than the asymptotic exponent of the pure model, $\nu_{\rm pure} = 1$, see (6), and vary with the degree of dilution. Note that similar values have been obtained before by using finite-size scaling [11]. However, those average values have been interpreted as reflecting logarithmic corrections to the power law of the perfect case [11]. Again, we

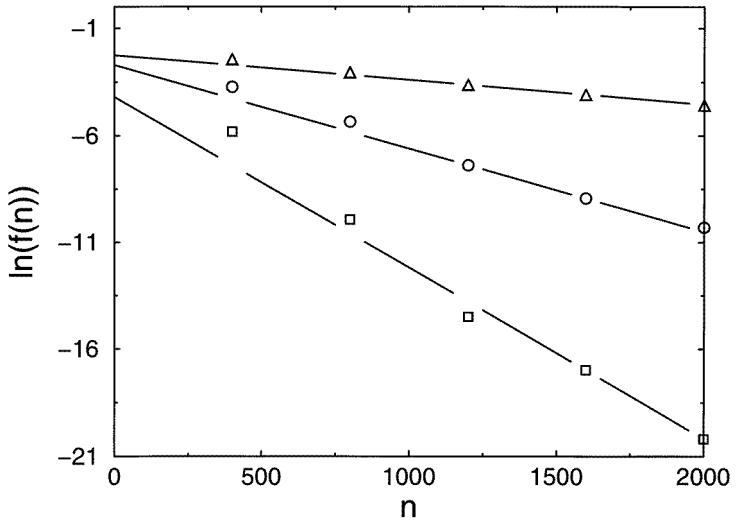

Figure 7. Finite iteration approximants to the surface magnetization, $f(n)$, as a function of n in a semi-logarithmic plot, at different reduced temperatures $t = 0.1$ (triangles), $t = 0.2$ (circles) and $t = 0.3$ (squares) above the critical point of the two-dimensional random Ising model with $r = \frac{1}{10}$. The slope of the curves, indicated by straight lines, corresponds to the inverse square of the average correlation length, see equation (19).

cannot rule out that possibility.

For further interpretation of our data, we consider the scaling relation [17]

$$\beta_1 = \nu\eta_\parallel/2 \tag{23}$$

which is satisfied, within the errors of the estimates, by the average exponents, both for $r = \frac{1}{4}$ and $r = \frac{1}{10}$. Following the alternate interpretation involving logarithmic corrections, the critical surface correlations, described by $\eta_\parallel$, would then be affected by logarithmic corrections, due to the correction terms in the correlation length (and their presumed absence in the surface magnetization). The above scaling law, (23), can be obtained by relating the surface correlation function between two spins at a distance of the correlation length, $\xi(t)$, to the square of the surface magnetization,

$$G_s(\xi(t)) \sim m_1^2(t) \tag{24}$$

in the limit $t \to 0$ (when logarithmic corrections are present, such a relation has been, for instance, checked for the $q = 4$ state Potts model [28]). Then, supposing logarithmic terms in the surface correlations, but not in the surface magnetization, one easily arrives at the conjecture

$$G_s(l) \sim l^{-1}(\ln l)^{1/2}. \tag{25}$$

4. Summary

In this paper, the boundary critical properties of the two-dimensional random Ising model have been studied by MC techniques and by the ST approach. In the simulations, we computed magnetization profiles, allowing us to monitor surface and bulk quantities simultaneously. On the other hand, by the ST method we calculated the surface magnetization as well as surface correlation functions. Both methods provide data for

the surface magnetization which are in very good agreement, demonstrating the correctness and accuracy of the two approaches.

To analyse the behaviour of the random Ising model in the critical region, we considered three singular quantities: the surface magnetization, the (surface) correlation length and the critical surface correlation function. The surface magnetization of the dilute model, as obtained from both methods, follows closely the power law of the corresponding perfect model, where $\beta_1 = \frac{1}{2}$, showing the robustness of that exponent against even fairly strong randomness.

The behaviour of the other two singular quantities, the critical surface correlation function and the correlation length, as determined from the ST method, is rather subtle. Note that in the ST method we averaged over the *logarithm* of the surface correlation function, leading to information about the *typical* behaviour of the correlation length. The numerical estimates for the critical exponents of both quantities, i.e. $\nu_\parallel$ and $\eta_\parallel$, are found to be dilution dependent, when calculating average exponents. Similar findings have been reported before for bulk exponents in the two-dimensional random Ising model. These non-universal average bulk exponents have been interpreted previously either as reflecting the true asymptotics (satisfying weak universality) or as being due to logarithmic corrections of the power laws in the perfect model (in accordance with field-theoretical predictions). Our numerical data for the surface quantities leave room for both types of interpretation, concerning bulk and surface critical properties. Extending the field-theoretical predictions and attributing the apparent variation of the average exponents with the degree of dilution to logarithmic corrections, we conjectured, in equation (25), the asymptotic form of the critical surface correlation function.

Note added in proof. Attention is drawn to a recent work suggesting $\beta_1 = 1/2$ for the two-dimensional Ising model with random couplings at the surface [29].

Acknowledgments

PL and FSz would like to thank the Institutes for Theoretical Physics at the Universität Hannover (especially Professor H U Everts) and the Technische Hochschule Aachen for kind hospitality, as well as the Deutsche Akademische Auslandsdienst and the Soros Foundation, Budapest, for facilitating their visits. FI's work has been supported by the Hungarian National Research Fund under grants OTKA TO12830 and OTKA TO23642 and by the Ministery of Education under grant no FKFP 0765/1997.

Appendix

We consider the first two layers of a hexagonal Ising lattice (figure 4), where a surface spin s is connected to the second layer spins s_+ and s_- by couplings p_+ and p_-, respectively. We are interested in a relation between the thermal averages $\langle s_+ \rangle$, $\langle s_- \rangle$ and $\langle s \rangle$.

We start by considering the conditional probability

$$P(s)|_{s_+,s_-} = \frac{\exp(p_+ s s_+ + p_- s s_-)}{\sum_s \exp(p_+ s s_+ + p_- s s_-)} \tag{26}$$

with fixed values of s_+ and s_-. Under this condition the expectational value of s is given by

$$\langle s \rangle|_{s_+,s_-} = \tanh(p_+ s_+ + p_- s_-)$$

$$= \tanh\left[(s_+ + s_-)\frac{p_+ + p_-}{2} + (s_+ - s_-)\frac{p_+ - p_-}{2}\right] \tag{27}$$

which can be evaluated using the fact that $s_+ = \pm 1$ and $s_- = \pm 1$ as

$$\langle s\rangle|_{s_+,s_-} = s_+\frac{\tanh(p_+ + p_-) + \tanh(p_+ - p_-)}{2} + s_-\frac{\tanh(p_+ + p_-) + \tanh(p_- - p_+)}{2}. \tag{28}$$

At this point, one can sum over the variables s_+ and s_- leading to

$$\langle s\rangle = \langle s_+\rangle\frac{\tanh(p_+ + p_-) + \tanh(p_+ - p_-)}{2} + \langle s_-\rangle\frac{\tanh(p_+ + p_-) + \tanh(p_- - p_+)}{2} \tag{29}$$

which is equivalent to equation (11).

The connected surface correlation function of the nth triangular model $g^{(n)}(i+l,i) = \langle s^{(n)}_{i+l}s^{(n)}_i\rangle - \langle s^{(n)}_{i+l}\rangle\langle s^{(n)}_i\rangle$ and that of the $(n+1)$th model are related by

$$\begin{aligned} g^{(n)}(i+l,i) = {} & a^{(n+1)}_{(i+l)+}a^{(n+1)}_{i+}g^{(n+1)}(i+l+1,i+1) + a^{(n+1)}_{(i+l)+}a^{(n+1)}_{i-}g^{(n+1)}(i+l+1,i-1) \\ & + a^{(n+1)}_{(i+l)-}a^{(n+1)}_{i+}g^{(n+1)}(i+l-1,i+1) + a^{(n+1)}_{(i+l)-}a^{(n+1)}_{i-}g^{(n+1)}(i+l-1,i-1) \end{aligned} \tag{30}$$

which can be obtained along the lines of (11). Iterating the expression in (30), one obtains a sum, each term of which can be formally represented by two directed walks, which start at positions $i+l$ and i, respectively. If the two walks meet at step n and at some position j, then $g^{(n)}(j,j) = 1 - \langle s^{(n)}_j\rangle^2$ and the walks annihilate each other. In the $n \to \infty$ limit, the non-vanishing contribution to $g^{(0)}(i+l,i) = g(i+l,i)$ is given by those processes, which are connected to annihilated walks. In the transfer matrix notation the average surface correlation function is given by

$$G_s(l) = \frac{1}{L}\sum_{i=1}^{L}\sum_{a.w.}\left[\prod_{m=1}^{n}\mathbf{A}^{(m)}\right]_{i+l,j}\left[\prod_{k=1}^{n}\mathbf{A}^{(k)}\right]_{i,j}[1 - (\sigma^{(n)}_j)^2]. \tag{31}$$

The asymptotic behaviour of this expression can be obtained by noting that the transverse fluctuations of directed walks have Gaussian nature, and the corresponding probability distribution is sharp. Consequently, in the large l (and large n) limit it is enough to consider the typical processes. Then there are two factors in (31), which are both approaching the partition function of n-step directed walks, $f(n)$, see (15), and these contributions should be multiplied by $P_n(l)$, the ratio of those walks which are annihilated at the nth step. In this way, we obtain

$$G_s(l) \approx \sum_n P_n(l)[f^2(n) - f^2(\infty)] \tag{32}$$

which in the continuum approximation is given in (17).

References

[1] Harris A B 1974 *J. Phys. C: Solid State Phys.* **7** 1671

[2] Dotsenko Vik S and Dotsenko Vl S 1983 *Adv. Phys.* **32** 129
Dotsenko V 1995 *Usp. Fiz. Nauk* **165** 481

[3] Shalaev B N 1994 *Phys. Rep.* **237** 129

[4] Selke W, Shchur L N and Talapov A L 1994 *Annual Reviews of Computational Physics* vol 1, ed D Stauffer (Singapore: World Scientific) p 17

[5] Dotsenko V, Picco M and Pujol P 1995 *Nucl. Phys.* B **455** [FS] 701

[6] Ludwig A W W 1990 *Nucl. Phys.* B **330** 639
[7] Wang J-S, Selke W, Dotsenko Vl S and Andreichenko V B 1990 *Physica* **164A** 221
[8] Ballesteros H G, Fernandez L A, Martin-Mayor V, Muñoz Sudupe A, Parisi G and Ruiz-Lorenzo J J 1997 *J. Phys. A: Math. Gen.* **30** 8379
[9] de Queiroz S L A and Stinchcombe R B 1996 *Phys. Rev.* E **54** 190
[10] Stauffer D, Aarão Reis F D A, de Queiroz S L A and dos Santos R R 1997 *Int. J. Mod. Phys.* C **8** 1209
[11] Aarão Reis F D A, de Queiroz S L A and dos Santos R R 1997 *Phys. Rev.* B **56** 6013
[12] Kim J-K and Patrascioiu A 1994 *Phys. Rev. Lett.* **72** 2785
[13] Kühn R 1994 *Phys. Rev. Lett.* **73** 2268
[14] Mc Coy B M and Wu T T 1973 *The Two-dimensional Ising Model* (Cambridge: Harvard University Press)
[15] Selke W, Szalma F, Lajkó P and Iglói F 1997 *J. Stat. Phys.* **89** 1079
[16] Fisch R 1978 *J. Stat. Phys.* **18** 111
[17] Binder K 1983 *Phase Transitions and Critical Phenomena* vol 8, ed C Domb and J L Lebowitz (London: Academic) p 1
[18] Diehl H W 1986 *Phase Transitions and Critical Phenomena* vol 10, ed C Domb and J L Lebowitz (London: Academic) p 75
[19] Bariev R Z 1980 *Teor. Mat. Fiz.* **40** 95
[20] Czerner P and Ritschel U 1997 *Int. J. Mod. Phys.* B **11** 2075
[21] Fisher M E and Ferdinand A E 1967 *Phys. Rev. Lett.* **19** 169
[22] Peschel I 1984 *Phys. Rev.* B **30** 6783
[23] Pleimling M and Selke W 1998 *Eur. Phys. J.* B **1** 385
[24] Hilhorst H J and van Leeuwen J M J 1981 *Phys. Rev. Lett.* **47** 1188
[25] Burkhardt T W, Guim I, Hilhorst H J and van Leeuwen J M J 1984 *Phys. Rev.* B **30** 1486
[26] Iglói F and Lajkó P 1996 *J. Phys. A: Math. Gen.* **29** 4803
[27] Burkhardt T W and Guim I 1998 *Physica* A in press
[28] Cardy J L, Nauenberg M and Scalapino D J 1980 *Phys. Rev.* B **22** 2560
[29] Diehl H W 1998 *Eur. Phys. J.* B **1** in press